Electronic Supplementary Material (ESI) for Nanoscale.

Supporting Information

Monitoring of single and double lipid membrane formation with high spatiotemporal resolution using evanescent light scattering microscopy

Björn Agnarsson[1], Hannah Wayment-Steele[2], Fredrik Höök[1], and Angelika Kunze[1,3,*]

[1]Department of Applied Physics, Chalmers University of Technology, 412 96 Göteborg, Sweden

[2]Department of Chemistry, Pomona College, 645 North College Ave. Claremont, CA 91711, USA

[3]Institute of Physical Chemistry, University of Göttingen, 37077 Göttingen, Germany

Experimental Section

Chemicals

1-Palmitoyl-2-oleoyl-*sn*-glycero-3-phosphocholine (POPC) and 1-palmitoyl-2-oleoyl-*sn*-glycero-3-phospho-(1'-*rac*-glycerol) (POPG) were purchased from Avanti Polar Lipids Inc. (AL, USA). 1,2-dioleoyl-*sn*-glycero-3-phosphoethanolamine (DOPE) labeled with ATTO488 dye was purchased from ATTO-TEC GmbH (Germany). All other chemicals were obtained from commercial sources and used without further purification. Water was deionized (resistivity > 18 $M\Omega \cdot cm^{-1}$) and purified using a MilliQ unit (MilliQ plus, Millipore, France). TRIS buffer (pH 8) contained 10 mM TRIS and 100 mM NaCl. TRIS-$CaCl_2$ and TRIS-$AlCl_3$ buffers were made from TRIS buffer supplemented with 10 mM $CaCl_2$ and 10 mM $AlCl_3$, respectively. Buffers were filtered, using 25 mm PVDF membrane filters with 0.2 µm pore size, and degassed before use.

Vesicle preparation

Lyophilized lipids were dissolved in chloroform (stock solutions were stored at -20°C) and placed with the desired ratio in round bottom flasks. The solvent was first evaporated under a gentle stream of nitrogen while gently turning the flask to form a thin lipid film onto the wall of the flask, and then further dried under vacuum for 3 hours. The lipid films were hydrated in TRIS-buffer. After vortexing, the solutions were extruded 13 times through 30 nm filters (Nucleopore Track-Etched Membrane, Whatman, USA). Vesicles prepared in this way typically measure around 100 nm in diameter, as determined by dynamic light scattering and nanoparticle tracking analysis. The vesicle solutions were stored refrigerated under nitrogen.

QCM-D

QCM-D experiments were performed using a Q-Sense E4 instrument (Q-Sense AB, Sweden). AT-cut quartz crystals with a fundamental frequency of 5 MHz coated with SiO_2 were purchased from Q-Sense AB. Prior to experiment, the crystals were cleaned in a 10 mM sodium dodecyl sulfate aqueous (SDS) solution (overnight), rinsed thoroughly with water, dried under nitrogen, and treated with UV/ozone for 3 x 15 min with rinsing with water and drying in between. Measurements were carried out at 22°C using a constant flow rate of 100 µl/min. Frequency and dissipation shifts were measured at the seventh harmonic. Frequency shifts were normalized to the fundamental frequency by dividing the values by 7.

SPR

SPR measurements were carried out using a BioNavis 220A NAALI instrument (BioNavis, Finland) and silica coated sensor slides. The slides were thoroughly cleaned using 10 mM SDS and then kept in SDS over night. Prior to experiments the slides were rinsed using deionized water before being dried under nitrogen and

treated with UV/ozone for 15 min. Angular scan measurements were carried out at 22 °C using a constant flow rate of 30 µl/min.

Fluorescence recovery after photobleaching (FRAP)

FRAP experiments were carried out employing an Olympus X61 microscope equipped with a 100 W mercury lamp using a 100X, NA = 1 water immersion objective. Prior to bleaching, 3 images of the SLM were acquired to compensate for uneven illumination over the sample. Thereafter a circular spot (45 µm in diameter) was bleached for 60 s using maximum intensity of the mercury lamp followed by a series of 60 images taken at 2 s intervals with lowered intensity of the mercury lamp. Diffusion was determined from three discrete spots on each SLM. Image analysis was performed using the Matlab script "frap-analysis" described in detail by Jonsson et al.[1]

EvSM chips

A single-mode, symmetric planar waveguide structure consisting of a 500 nm thick silica core layer (spin-on-glass, IC1-200 from Futurrex Inc.) embedded in a 7 µm thick cladding layer of a fluorinated polymer (CYTOP, CTX-809AP2 from AGC Chemicals, ASAHI Glass Co., LTD.) was fabricated on a standard Si(100) 4" wafer by spin-casting at the MC2 nanofabrication laboratory, Chalmers, Sweden (Fed. Std.209 E 10-100). A pattern, consisting of 2x2 mm^2 openings (sample wells), were formed in the upper cladding layer by reactive ion etching, exposing the core layer of the waveguide to the environment. A thick protective layer of photoresist was then spin-cast on the wafer. The wafer was diced into 1x1 cm^2 chips, with each chip containing a single sample well at its middle.

The protective photoresist was removed using appropriate photoresist remover followed by a gentle rinsing in deionized water for 5 minutes. The chips were then blow-dried using nitrogen and stored in a cupboard until intended use. Prior to use, the chips were treated with low power O_2 plasma for 10 minutes before being placed under the microscope with a drop of the appropriate buffer solution placed in the sample well of the chip.

A TE polarized 488 or 532 nm light was coupled into the chip using end-fire coupling from a single mode optical fiber aligned to the facet of the chip. Same fiber was used for both wavelengths. The light in the core layer of the waveguide generates an evanescent light that extends approximately δ = 110 nm into solution from the silica surface of the sample well of the chip[2]. Objects within this 110 nm sensing depth, such as adsorbing vesicles, will scatter the evanescent light, which then is collected directly using a standard water immersive objective.

[1] Jönsson, P., Jonsson, M. P., Tegenfeldt, J.O., Höök, F. *Biophys. J.* **95,** 5334- 5348 (2008).

[2] The extension, δ, of the evanescent light intensity is here defined using the relation $I(z) = I_0 e^{-z/\delta}$, where I_0 is the intensity at surface (z = 0) and $I(z=\delta) = I_0/e$.

EvSM and dual-mode EvSM set-up

The experiments were carried out employing an Olympus X61 microscope equipped with a 100 W mercury lamp using a 100X, NA = 1 water immersion objective. All measurements were carried out at room temperature. Two cameras were used for acquiring data, a Hamamatsu ORCA Flash 4.0 V2 CMOS camera 2048×2048 and an Andor Luca 512×512 EM-CCD. The particular choice of camera used was depended only on what was available for use at each time. EvSM scattering data was acquired using the 532 nm green laser in combination with a FITC filter cube (U-MWIBA3, excitation band pass filter 460-495 nm, dichroic mirror at 505 nm and emission band pass filter 510-550 nm), which transmits the scattered light.

Epi-fluorescence measurements where carried out using the same filter and a mercury short arc lamp for excitation.

Using an image splitter (OptoSplit II, image splitter from Andor) the adsorption of POPG vesicles supplemented with 0.1 % labeled vesicles (POPG:DOPE-Atto488, 98:2) could be monitored simultaneously in bright field (scattering) and fluorescence. The scattering and fluorescence excitation was generated using a 488 nm laser and using the same FITC filter cube. With the image splitter the imaging sensor was divided into two parts, one showing the scattered blue light and on the other half the fluorescent green light.

Result Section

EvSM – POPC vesicle adsorption and SLM formation

Movies showing different kinetics of a SLM formation using EvSM were acquired. The movies all show POPC membrane formation in TRIS.

Movie SM1

SLM formation used for the analysis presented in Fig. 2 in the main article, acquired at 2 frames per second, 1×1 binning, with the EM-CCD Andor Luca camera with gain set to 200 and exposure time to 100 ms. Field of view is 75×75 μm^2. POPC vesicles concentration is approximately 0.5 mg/ml.

Movie SM2

SLM formation acquired at 1 frame per 2 seconds using Hamamatsu ORCA Flash 4.0 V2 CMOS camera, 2×2 binning and 50 ms exposure. Field of view is 100×100 μm^2. The movie shows the edge between the silica sensing well (left part of the frame showing adsorbed POPC vesicles) and the CYTOP cladding layer (right half of the image, showing no POPC vesicles). POPC vesicle concentration is approximately 0.3 mg/ml.

Movie SM3

SLM formation using a lower concentration of POPC vesicles, resulting in membrane patches forming simultaneously on the surface, which then fuse together to from a homogenous SLM. The movie is acquired using Hamamatsu ORCA Flash 4.0 V2 CMOS camera at 1 frame per second, 2×2 binning and 50 ms exposure. Field of view is 122×122 μm^2. The movie starts a few seconds into the process with a few vesicles already adsorbed on the surface. Vesicle concentration is approximately 0.1 mg/ml.

Movie SM4

SLM formation acquired at 1 frame per 2 seconds using Hamamatsu ORCA Flash 4.0 V2 CMOS camera, 1×1 binning and 50 ms exposure. Field of view is 80×80 μm^2. POPC vesicle concentration is approximately 0.3 mg/ml.

EvSM – POPC/POPG vesicle adsorption and SLM

Figure S1 shows a typical formation of POPC/POPG SLM. Vesicles composed of 50 wt% POPC and 50 wt% POPG were injected to the chip at t = 80 s. Similar to the described formation of the POPC SLM, the mean frame intensity increased until the critical coverage with intact vesicles was reached (intensity plateau at t = 450 s) followed by a decrease in intensity indicating rupture and fusion of liposomes.

Movies were acquired for the POPC/POPG vesicle adsorption and subsequent bilayer formation in TRIS-$CaCl_2$ buffer.

Movie SM5

The POPC/POPG SLM formation used to generate Fig. S1. The movie is acquired at 1 frames per 2 seconds, 2×2 binning, using the Hamamatsu ORCA Flash 4.0 V2 camera

with exposure time set to 50 ms. Field of view is 122×122 μm^2. Vesicle concentration is approximately 0.2 mg/ml.

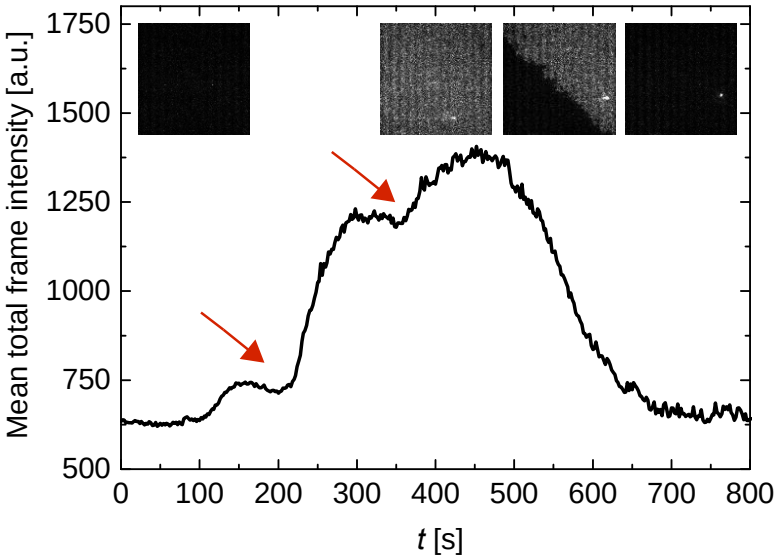

Figure S1 Label-free imaging of POPC/POPG SLM formation. The graph shows the mean frame-intensity from a 122×122 μm^2 area on the sensing region of the EvSM chip upon injection of POPC/POPG (50:50) vesicles (100 nm) in TRIS-$CaCl_2$ buffer. Initially, the chip is exposed to a buffer solution with the surface only showing a few stray scattering objects (first photo inset). As vesicles are injected (t = 80 s) to the buffer solution they are observed to adsorb on the surface resulting in a steady increase of the mean frame intensity. After approximately 450 s a maximum in the mean frame intensity is reached indicating maximum vesicle surface coverage. At this point the vesicles rupture and fuse together to form a homogenous SLM in a wave-like fashion (third photo inset) resulting in a steady decrease in the mean frame intensity until a plateau is reached at the completion of the membrane formation. Red arrows indicate time of mixing.

Dual-mode EvSM – POPG vesicle adsorption and formation of the DLM

Movie SM6 shows the initiation of the POPG:DOPE-Atto488 vesicle rupture process and the formation of DLM by changing buffer from TRIS to 10 mM TRIS-$AlCl_3$. The scattering channel (left) shows only large scattering signal with no possibility of single vesicle detection while the fluorescence channel (right) shows how 1 of every 1000 adsorbed vesicles starts to rupture and incorporate their fluorescently labeled lipids into the DLM.

Movie SM6

DLM formation used for the analysis presented in Fig. 4 in the main article. Images were acquired using Hamamatsu ORCA Flash 4.0 V2 CMOS camera, 1×1 binning and 500 ms exposure.

Membrane morphology with EvSM.

EvSM revealed that the surface morphology of the SLMs differed between experiments using different lipid compositions and buffers. During membrane formation, occasionally, patches of intact vesicles could be observed (indicated by red arrows in Fig. S2a). These areas could in most cases be forced to form SLMs by

subjecting the surface to osmatic stress (for example by changing to deionized water and then back to the previous buffer). However, in case of POPC/POPG membranes highly scattering objects evenly distributed over the whole surface could be observed after SLM formation (see top micrograph in Fig. S2a). Upon removal of the Ca^{2+} by thoroughly rinsing with TRIS, these scattering objects disappeared. This observation would suggest these bright spots to be vesicles bound to the SLM with Ca^{2+} bridging between the negatively charged lipid headgroups of the SLM and the vesicles. However, when Ca^{2+} is again added to solution the scattering objects recur. Repeating buffer changes show that the formation of the scattering objects is reversible. In a recent study employing QCM-D and reflectometry we found that Ca^{2+} has reversible effects on PG containing SLMs.[3,4] In short, the bivalent cation was found to induce reversible structural changes and to reversibly affect the interfacial water layer. In the current study, the bright spots originate from an optical dense region either on top of or within the membrane itself. We already excluded vesicles to be the origin. Another cause for the spots could be small, densely packed domains or a folding of the SLM. The latter, however, can be excluded, as folding would only be expected to occur in TRIS, when the lipids are not as densely packed as in TRIS-$CaCl_2$.[8]

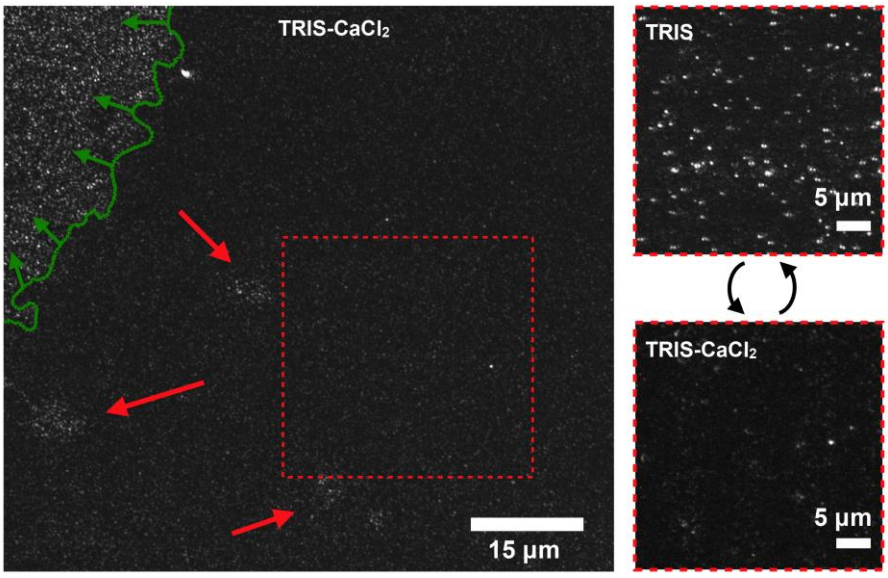

Figure S2 EvSM of POPG/POPC SLM formation, surface defects and the effect of buffer change. In some cases, after the membrane front had moved from a defect-free SLM area through that of highly concentrated absorbed vesicles (front and direction of movement indicated by green contour and arrows), areas imbedded in the SLM containing intact vesicles could be observed (indicated by red arrows). Upon changing the buffer from TRIS-$CaCl_2$ to TRIS, highly scattering spots were seen forming (upper micrograph of the area indicated by a red box). When changing back to TRIS-$CaCl_2$ these bright spots were removed (lower micrograph showing the same area). This process was reversible.

As described in the main text of the article (Fig. 3), the changing from TRIS to TRIS-$AlCl_3$ buffer after formation of the SLM resulted in a large increase in surface scattering. We argue that this increase related to increased optical density of the

[3] Kunze, A.; Zhao, F.; Marel, A.-K.; Svedhem, S.; Kasemo, B. *Soft Matter* **2011**, *7*, 8582

[4] Wayment-Steele, H.K.; Jing, Y.; Swann, M.J.; Johnson, L.E.; Agnarsson, B.; Svedhem, S.; Johal, M.S.; Kunze, A. *Langmuir* **2016**, *32*, 1771

SLM (more densely packed lipids) either due to domain formation and/or due to incorporation of Al^{3+}-ions in the SLM. When 10 mM TRIS-$AlCl_3$ buffer was used, this transition between normal and dense state was very fast (in the order of 1 s), while if lower concentrations were used, it became possible to follow the dynamics of this change (see Fig. S3), which seemed to occur in an avalanche-like fashion. As discussed in the main text, the SLM became totally immobile after this and regained only partial mobility after rinsing in TRIS buffer.

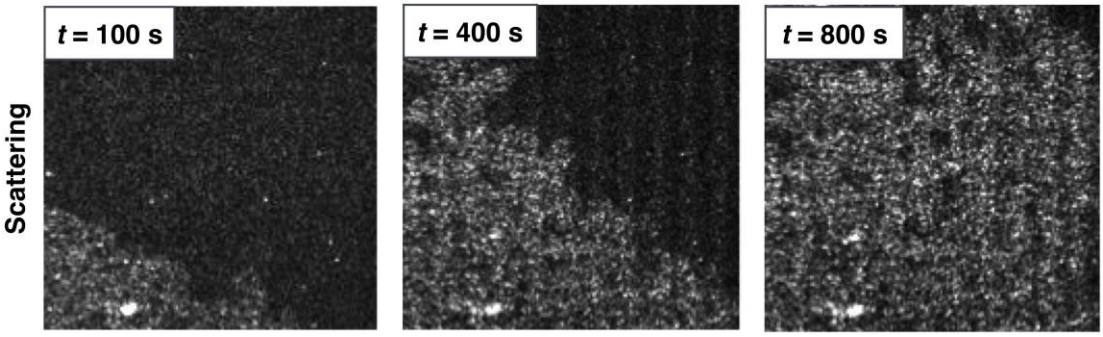

Figure S3 EvSM of POPG/POPC SLM subjected to TRIS-$AlCl_3$ buffer. When POPG/POPC SLM was subjected to low concentrations (< 1mM) TRIS-$AlCl_3$ buffer, the transition from normal SLM to optically dense membrane could be followed dynamically (Images are approximately 100×100 μm^2). (Images are approximately 40×40 μm^2).

SPR experiments of the stepwise DLM formation

To further support our claim for the formation of a DLM, measurements were carried out using dual-wavelength SPR. A formalism describing the use of dual wavelength SPR to determine the thickness of thin biomolecular films has been previously proposed by Rupert et al.[5] One of the results derived by Rupert et al. was that irrespective of whether measuring continuous films or non-deforming shell-like structures like lipid vesicles, the ratio between the two signal responses, *R*, can be expresses as

$$\frac{R_{\lambda_1}}{R_{\lambda_2}} = \frac{S_{\lambda_1}(dn/dC')_{\lambda_1}\delta_{\lambda_2}\phi(d_f/\delta_{\lambda_1})}{S_{\lambda_2}(dn/dC')_{\lambda_1}\delta_{\lambda_1}\phi(d_f/\delta_{\lambda_2})} \qquad \text{S(1)}$$

where *S* represents a sensitivity factor, usually expressed in measured SPR signal per change in bulk refractive index unit (RIU), (*dn/dC'*) is the derivative of the refractive index with respect to the molecule concentration in solution, δ_λ is the decay length of the exponentially vanishing SPR evanescent field and

$$\phi(d_f/\delta_\lambda) = [1 - exp(-d_f/\delta_\lambda)]\delta_\lambda/d_f \qquad \text{S(2)}$$

is a dimensionless factor that accounts for the interplay between the film/vesicle thickness/diameter, d_f, and the evanescent decay length, δ. In the limit $d_f << \delta$ (as is

[5] Rupert, D.L.M.; Shelke, G.V.; Emilsson, G.; Claudio, V.; Block, S.; Lässer, C.; Dahlin, A.; Lötvall, J. O.; Bally, M.; Zhdanov, V.P.; Höök, F., *Anal. Chem.* **2016**, *accepted*. DOI 10.1021/acs.analchem.6b01860

the case for SLM) this factor becomes close to unity which means that expression S(1) can be simplified to

$$\frac{R_{\lambda_1}}{R_{\lambda_2}} = \frac{S_{\lambda_1}(dn/dC')_{\lambda_1}\delta_{\lambda_2}}{S_{\lambda_2}(dn/dC')_{\lambda_2}\delta_{\lambda_1}}. \qquad \text{S(3)}$$

In our setup, $\lambda_1 = 670$ nm and $\lambda_2 = 785$ nm. The ratio of the sensitivity factors had previously been determined for the particular silica coated sensors used here to be $S_{\lambda_1}/S_{\lambda_2} = 1.19$ and similarly the ratio of decay lengths of the evanescent fields had been determined to be $\delta_{\lambda_2}/\delta_{\lambda_1} = 154/109 = 1.415$. Assuming that lipids have a similar refractive index dispersion as proteins[6] $(dn/dC)_{\lambda_1} \approx 1.012(dn/dC)_{\lambda_2}$, equation S(3) will yield $R_{\lambda_1}/R_{\lambda_2}$= 1.70, which, when substituted into equation S(1), makes it possible to use S(1) to plot the relation between the response ratio and film/vesicle thickness/diameter (solid curve in Fig. S4).

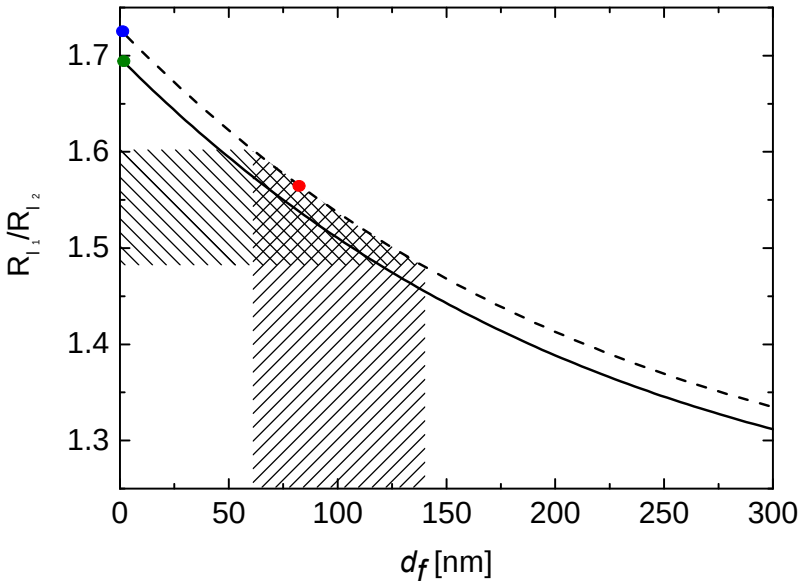

Figure S4 $R_{\lambda_1}/R_{\lambda_2}$ vs. d_f according to equation S(1) with the ratios in equation S(3) set to 1.70 (solid line) and 1.73 (dashed line). The green filled circle indicates the response ratio for a SLM in TRIS buffer ($R_{\lambda_1}/R_{\lambda_2}$= 1.70) and the blue circle the corresponding ratio after exposure to TRIS-$AlCl_3$ and subsequent rinsing in TRIS ($R_{\lambda_1}/R_{\lambda_2}$= 1.73). The filled shaded area indicates the distribution in POPG vesicles diameters and how it matches the measured response ratio of the adsorbed vesicles to the Al^{3+} treated SLM (red circle at $R_{\lambda_1}/R_{\lambda_2}$= 1.57). After exposing the adsorbed POPG vesicles to TRIS-$AlCl_3$ and after subsequent rinsing in TRIS the response ratio returns to $R_{\lambda_1}/R_{\lambda_2}$= 1.73 (blue circle $R_{\lambda_1}/R_{\lambda_2}$= 1.73).

The observed response ratio of 1.70 obtained for the POPC/POPG SLM formed in TRIS-$CaCl_2$ and subsequently rinsed in TRIS (see Fig. S5a) is in excellent agreement with the predicted ratio according to equation S1 (green circle in Fig. S4).

[6] Perlmann, G. E.; Longsworth, L. G. *J. Am. Chem. Soc.* **1948**, *70*, 2719**.**

Upon incubating with TRIS-$AlCl_3$ the SPR response from the POPC/POPG SLM is moderately affected, with the ratio $R_{\lambda_1}/R_{\lambda_2}$ slightly rising and leveling off at $R_{\lambda_1}/R_{\lambda_2}$ = 1.73 after a rinsing in TRIS (see Fig. S5a). This slight rise can be attributed to the irreversibly induced changes caused by the Al^{3+} ions on both the membrane and silica surface underneath. However, since the thin-film limit still applies, equation S(3) is still valid, but now resulting in a ratio $R_{\lambda_1}/R_{\lambda_2}$ = 1.73 (blue circle in Fig. S4) which, when substituted into equation S(1), will reveal a slightly shifted response ratio curve (dashed curve in Fig. S4).

After subsequent incubation with POPG vesicles, which adsorb on the SLM without spontaneously forming a bilayer, a response ratio of $R_{\lambda_1}/R_{\lambda_2}$ = 1.57 is measured (Fig. S5b). Comparing this value with the curves in Fig. S4 this ratio corresponds to an average film/vesicle thickness/diameter of around 85 nm (red filled circle in Fig. S4). Taking into account that the POPG vesicles will deform as they electrostatically adsorb to the SLM,[7] this value is in good agreement with what should be expected for adsorbed POPG vesicles with diameters in the 100 nm range and, more importantly, a clear indication of a layer consisting of unruptured vesicles.

Finally after exposing the adsorbed POPG vesicles to TRIS-$AlCl_3$ and rinsing with TRIS an increase in the response ratio back to 1.73 is observed, indicating rupture of vesicles and a formation of a second membrane fulfilling the thin film regime (see Fig. S5b and blue circle in Fig. S4).

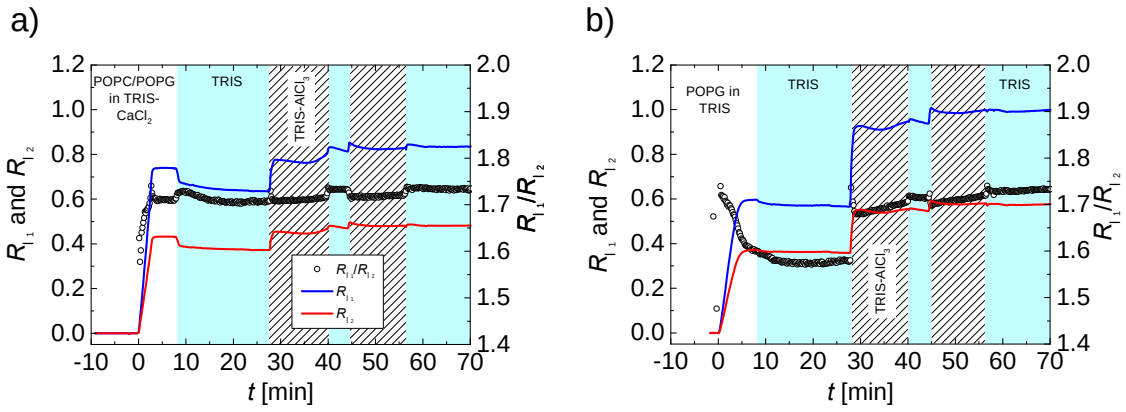

Figure S5 Dual wavelength SPR sensograms showing the SPR angle shift, *R*, versus time (blue: λ_1 = 670 nm; red: λ_2 = 785 nm) upon subsequent additions of a) 0.1 mg/ml POPG/POPC in TRIS-$CaCl_2$, followed by a injection of 10 mM TRIS-$AlCl_3$ and rinsing with TRIS and b) subsequent addition of 0.1 mg/ml POPG in TRIS on the Al^{3+}-treated SLM followed by injection of 10 mM TRIS-$AlCl_3$. Also shown are the corresponding $R_{\lambda_1}/R_{\lambda_2}$ ratios versus time (open grey circles). The shaded blue areas represent rinsing in TRIS and the patterned grey areas represent treatment with TRIS-$AlCl_3$.

QCM-D experiments showing stepwise formation of the double membrane

In addition to EvSM, fluorescence microscopy and dual wavelength SPR, QCM-D experiments of the stepwise formation of the DLM were performed. Fig. S6 shows QCM-D frequency and dissipation shift of the formation of SLM and subsequently a second membrane on top of that.

[7] Faiss, S.; Lüthgens, E.; Janshoff, A. *Eur. Biophys. J.* **2004**, *33*, 555.

In the first step a negatively charged SLM is formed on the negatively charged SiO_2 surface of a QCM-D crystal by adsorption and subsequent rupture of vesicles containing 50 wt% POPC and 50 wt% POPG in TRIS buffer (10 mM, 100 mM NaCl, pH 8) containing Ca^{2+}-ions (10 mM $CaCl_2$) (TRIS-$CaCl_2$) acting as bridging-ions between the SLM and the substrate. The SLM formation leads to the characteristic frequency shift of Δf = -26 Hz and dissipation shift of $\Delta D < 0.5 \cdot 10^{-6}$.[8] In the next step, the SLM is rinsed with TRIS, resulting in a dissipation shift of $\Delta D \sim 4 \cdot 10^{-6}$ whilst the frequency remains almost unchanged. As previously reported, this behavior can be attributed to structural changes within the bilayer and changes of the coupling/interaction with the underlying substrate.[9,10]

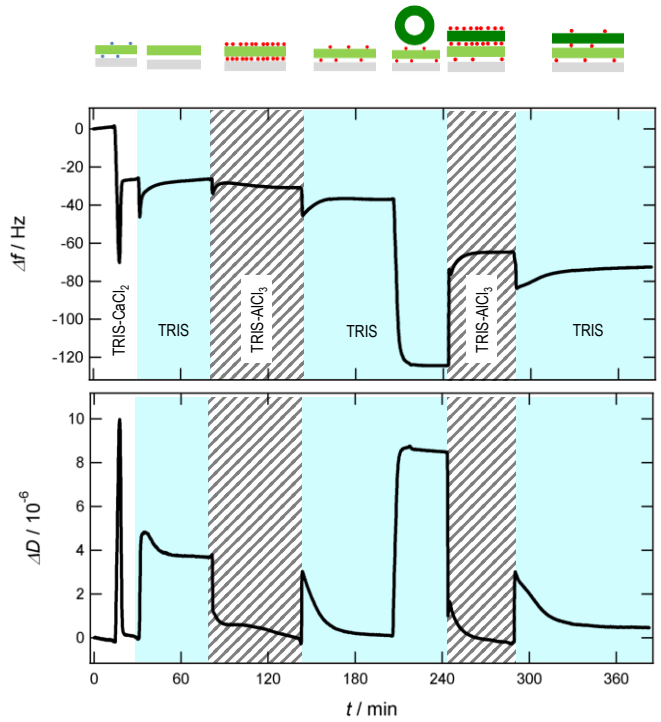

Figure S6 QCM-D frequency (top) and dissipation (bottom) shifts and schematic illustration of the stepwise formation of double membrane. Formation of a POPC/POPG (50:50) SLM (light green) in TRIS-$CaCl_2$ and subsequent buffer changes to TRIS, TRIS-$AlCl_3$, TRIS, addition of POPG (dark green) vesicles in TRIS, buffer change to TRIS-$AlCl_3$ and TRIS. Ca^{2+}-ions are indicated by blue dots and Al^{3+}-ions by red dots.

Upon injection of TRIS containing 10 mM $AlCl_3$, the dissipation decreases to a similar value as observed in TRIS-$CaCl_2$, whilst the frequency remains essentially constant. This indicates that Al^{3+} binds to the SLM in a similar manner as Ca^{2+}, acting as bridging molecules between the negatively charged SiO_2 surface and the SLM. However, upon changing buffer back to TRIS, the QCM-D signals remains essentially constant, indicating that Al^{3+}-ions bind, at least partially, irreversibly to the SLM, and thereby change the surface-charge of the membrane from being net negative to net

[8] Keller, C. A.; Kasemo, B. *Biophys. J.* **1998**, *75*, 1397

[9] Kunze, A.; Zhao, F.; Marel, A.-K.; Svedhem, S.; Kasemo, B. *Soft Matter* **2011**, *7*, 8582

[10] Wayment-Steele, H.K.; Jing, Y.; Swann, M.J.; Johnson, L.E.; Agnarsson, B.; Svedhem, S.; Johal, M.S.; Kunze, A. *Langmuir* **2016**, *32*, 1771

positive. The formation of the second membrane is achieved by injection of negatively charged vesicles (100% POPG) in TRIS to the, at this stage, net positively charged SLM. In the QCM-D signal (Fig. S6), this step results in a large drop of the frequency, accompanied by an increase of the dissipation, indicating the adsorption of intact vesicles onto the SLM. Vesicle rupture and formation of a second membrane is induced by changing buffer from TRIS to TRIS-$AlCl_3$. This results in a positive change in frequency and a negative shift in dissipation that stabilize at values corresponding to that of a double lipid membrane (Δf is double the value obtained for the single SLM in the corresponding buffer, ΔD is close to zero, see also Table S2).

QCM-D – addition of vesicles with varying fractions of charged lipids on top of the SLM

Experiments were performed where vesicles with varying fraction of negatively charged lipids were injected to the Al^{3+}-modified POPC/POPG SLM. Vesicles containing 100 wt% POPC, 80 wt% POPC + 20 wt% POPG, 50 wt% POPC + 50 wt% POPG, and 100 wt% POPG were probed. The resulting frequency and dissipation shifts of the vesicle adsorption in TRIS are shown Fig. S7 and listed in Table S1. For vesicles composed of 100 wt% neutral POPC, i.e. without negatively charged POPG, relatively small changes in frequency and dissipation were observed (incomplete surface adsorption). However, significant changes in the QCM-D signal were observed for the addition of all negatively charged liposomes (Table S1), indicating that the surface charge of the POPC/POPG SLM has changed due to irreversible binding of Al^{3+} turning the SLM from being net negatively charged into net positively charged.

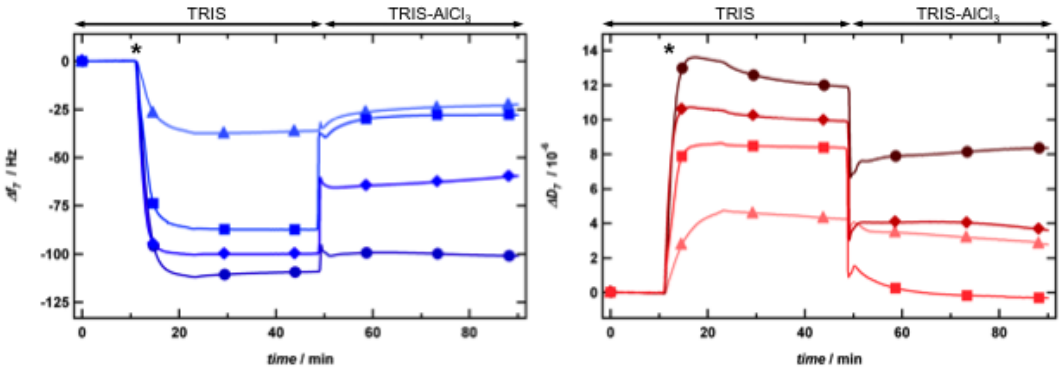

Figure S7 QCM-D frequency (blue, left hand side) and dissipation (red, right hand side) shifts for adsorption of vesicles containing different fractions of charged POPG in TRIS onto an Al^{3+} modified POPC/POPG SLM and subsequent injections of TRIS-$AlCl_3$. (triangle) POPC, (circle) 80 wt% POPC + 20 wt% POPG, (diamond) 50 wt% POPC + 50 wt% POPG, and (square) POPG. Injection of vesicles is indicated by a *.

Table S1 Mean values and the corresponding standard deviation of the frequency shift Δf and dissipation shift ΔD for adsorption of vesicles containing varying fractions of negatively charged POPG to the first membrane.

	Δf / Hz	ΔD / 10^{-6}
0% POPG	24 ± 10	3.4 ± 1.1
20% POPG	106 ± 4	13.2 ± 0.6
50% POPG	89 ± 11	10.2 ± 0.4
100% POPG	74 ± 11	7.8 ± 0.7

Vesicles containing different fractions (0 wt%, 20 wt%, 50 wt% and 100 wt%) of negatively charged POPG that had been adsorbed to the Al^{3+} modified POPC/POPG SLM, were exposed to TRIS-$AlCl_3$ buffer to induce vesicle rupture and formation of a second membrane. Table S2 summarizes the observed shifts in frequency and dissipation for the different vesicles prepared upon TRIS-$AlCl_3$ exposure.

Table S2 Mean values and the corresponding standard deviation of the frequency shift Δf and dissipation shift ΔD after injection of TRIS-$AlCl_3$.

	Δf / Hz	ΔD / 10^{-6}
0% POPG	22 ± 10	2.0 ± 1.6
20% POPG	116 ± 5	9.9 ± 1.3
50% POPG	54 ± 9	3.2 ± 0.3
100% POPG	29 ± 4	0.1 ± 0.5

Vesicles containing no or 20 wt% POPG showed little change upon Al^{3+} exposure, which suggests that no rupture occurred. Vesicles containing 50 wt% and 100 wt% POPG did demonstrate significant decreases in frequency and dissipation when Al^{3+} was added, suggesting vesicle rupture. However only liposomes containing 100 wt% POPG were observed to fully rupture and form a second membrane, as evidenced by the dissipation shift returning to 0 and the frequency shift decreasing by 29 Hz.